ISSN 0742-0463, Journal of Volcanology and Seismology, 2007, Vol. 1, No. 6, pp. 357–371. © Pleiades Publishing, Ltd., 2007.
Original Russian Text © E.V. Verzhbitskii, M.V. Kononov, V.D. Kotelkin, 2007, published in Vulkanologiya i Seismologiya, 2007, No. 6, pp. 3–18.

Geothermal Regime and Geodynamics of the North Pacific Ocean

E. V. Verzhbitskii[a], M. V. Kononov[a], and V. D. Kotelkin[b]

[a] *Institute of Oceanology, Russian Academy of Sciences, Moscow, 117997 Russia*
[b] *Faculty of Mechanics and Mathematics, Moscow State University, Moscow, 119899 Russia*

Received March 30, 2006

Abstract—The distribution of heat flow in the North Pacific Ocean has been examined, and a map of geothermal and geomagnetic fields for the Bering Sea as it is known today has been made. Reliable data are lacking regarding the time of origin for features of oceanic and continental genesis in the Bering Sea, which is an obstacle to the study of geodynamic processes in the North Pacific. Heat flow data were used to yield numerical estimates for the age of seafloor features in the Bering Sea: the Kamchatka Basin (21 Ma), Shirshov Ridge (95 Ma for the northern part and 33 Ma for the southern), the Aleutian Basin (70 Ma), Vitus Rise (44 Ma), Bowers Ridge (30 Ma), and Bowers Basin (40 Ma). These age estimates are corroborated by combined geological, geophysical, and plate kinematic data. A thermochemical model of global mantle convection has been developed in order to perform a numerical simulation of the thermal process involved in the generation of extended regional features in the North Pacific (the Emperor Fracture Zone, Chinook Trough, etc.). The modeling suggests a plume-tectonic origin for these features, yielding the optimal model for the tectonic evolution of the North Pacific. An integrated geological and geothermal analysis leads to the conclusion that the northern and southern parts of the Shirshov Ridge are different, not only in geologic age, but also in tectonic structure. The northern part is of imbricated-thrust terrane origin, while the southern part is of ensimatic island-arc origin, similar to that of Bowers Ridge. The seafloor of the Aleutian Basin is an outlier of the Upper Cretaceous Kula plate where, in the Vitus Rise area, backarc spreading processes originated during Eocene time. The terminating phase of activity in the Bering Sea began about 21 Ma by spreading in the older seafloor of the Kamchatka Basin. We developed plate-tectonic reconstructions of evolution for the North Pacific for the times 21, 33, 40, and 70 Ma in the hotspot system based on age estimates for the seafloor features derived from heat flow data and modeling of the thermal generation of regional faults, as well as on an analysis of geomagnetic, tectonic, and geological data.

DOI: 10.1134/S0742046307060012

INTRODUCTION

The North Pacific considered in this paper is east of the Hawaiian–Emperor seamount chains, and also includes the Bering Sea. The Hawaiian–Emperor chain extends for 6000 km and includes 107 individual volcanoes. The origin of these aseismic ridges is due to intraplate volcanism in the Pacific plate as it was passing over the Hawaiian hotspot plume. The Hawaiian Ridge and the Emperor seamount chain are, as a whole, in a zone of quiet magnetic field with no magnetic lineations. The interpolation of seafloor age using the magnetic anomalies situated about 2000 km from, and at an angle to, the trend of the ridges considerably complicates the identification of lithosphere age in the quiet magnetic zone [9]. The North Pacific has a complex tectonic structure and extends for more than 6000 km from the Hawaiian–Emperor seamount chain to the Surveyor, Mendocino, Pioneer, Murray, and Molokai fracture zones, as far as the North American Cordillera, and from the continental margin of the Aleutian Basin, as far as to the beginning of the Hawaiian Ridge in the Hawaiian plume area.

The Aleutian island arc separates the Bering Sea from the Pacific Ocean and extends for 2000 km from the Kamchatkskii Peninsula to Alaska (Fig. 1). The deeper part of the Bering Sea is divided by the aseismic Shirshov and Bowers ridges into the Kamchatka Basin, Aleutian Basin, and Bowers Basin. The necessary parameter for reconstructing the geological evolution of the North Pacific is the age of Bering Sea features [15, 39]. Special attention should be drawn to the fact that there are no reliable data on the basement age for various features in the Bering Sea characterized by continental and oceanic crust types. This considerably impedes the study of geodynamic processes in the North Pacific. Even now, the origin of several regional depressions in the North Pacific, such as the Emperor Fracture Zone, Chinook Trough, etc., is not sufficiently known. For example, the Emperor Fracture Zone is considered to be a major transform fault [48, 50] or as an older spreading center [60, 61]. This uncertainty in our knowledge of the origin of these structures considerably complicates the analysis of kinematic data, and accordingly, the development of plate tectonic recon-

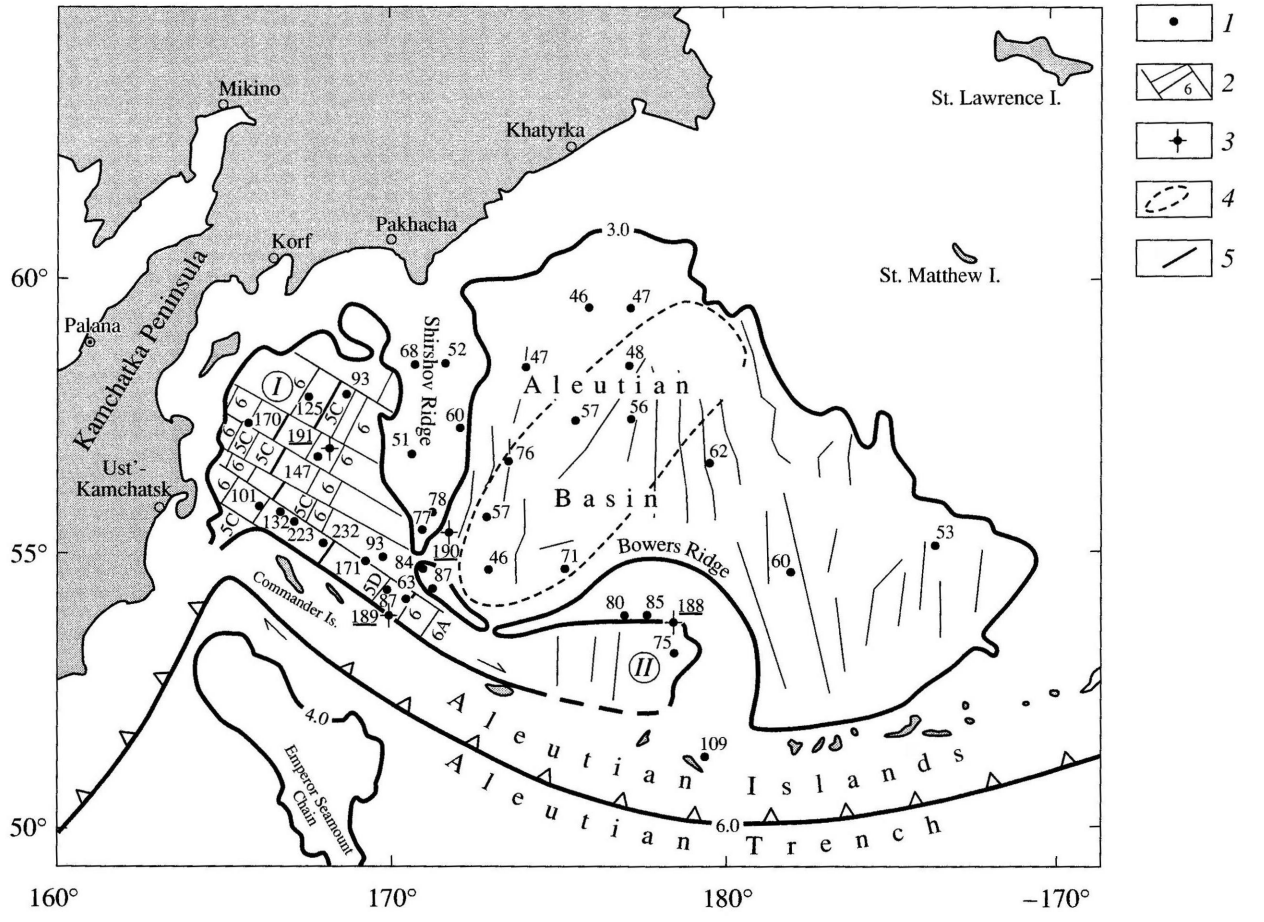


Fig. 1. A map of major features, geothermal and geomagnetic data for the Bering Sea: (*1*) heat flow in mW/m^2 after [4, 24], (*2*) axes of magnetic anomalies (with indication of anomaly number where known) and transform faults after [3, 27, 40], (*3*) deep-sea wells and well numbers (underlined in bold) after [64], (*4*) outline of Vitus Rise, (*5*) axial magnetic anomalies. Roman numerals denote basins: *I* Kamchatka Basin, *II* Bowers Basin. Solid lines show isobaths in km.

structions, and thus complicates the understanding of the entire region's evolution.

The present study examines geothermal and other geological and geophysical data, as well as the age patterns of intraplate hotspot magmatism, to calculate the ages of various structures in the Bering Sea, to do a numerical modeling of thermal conditions for the generation of long regional faults (the Emperor Fracture Zone, Chinook Trough, etc.), and to develop plate tectonic reconstructions for the evolution of the North Pacific at 21, 33, 40, and 70 Ma in the hotspot system.

THE AGE OF BERING SEA FEATURES FROM GEOTHERMAL DATA

The ages of Bering Sea features were calculated (Fig. 1), mostly from heat flow data to be found in [4, 10, 24, 28–31]. We also estimated corrections to measured heat flow values for sedimentation rate and the contrast in the heat conduction and thermal diffusivity between the sediment and the crystalline basement [12]. The estimates showed that the corrections did not exceed the uncertainty of geothermal measurements (10–15%) for the southwestern Kamchatka Basin, Bowers Basin, and the Shirshov and Bowers ridges, where the sediments are thin (1–2 km), and so the measured heat flow values have not been modified. As to the Aleutian Basin and Vitus Rise with thicker sediments, the measured heat flow has been accordingly corrected (see below).

The western Bering Sea is occupied by the Kamchatka Basin (Fig. 1), whose sediments are thinner than 2 km [4]. Magnetic lineations 6, 6A, 5D, and 5C (21–17 Ma, Early Miocene [3]) were identified in the southwestern Kamchatka Basin. Figure 2 shows the distribution of measured heat flow across the axis of opening for the southwestern Kamchatka Basin [7, 24, 27].

The geothermal model describes the cooling of the oceanic lithosphere by the relation (the theoretical geothermal curve) [38, 58]

$$q = \frac{\lambda T_a}{\sqrt{\pi a t}} = 480/\sqrt{t}, \qquad (1)$$

where q mW/m^2 is the heat flow, $\lambda = 3.2 \times 10^3$ mW/(m^2 K) is the thermal conductivity of lithospheric material, T_a = 1350°C is the temperature in the asthenosphere, $a = 8.0 \times 10^{-7}$ m^2/s is the thermal diffusivity of mantle material, and t Myr is the age of the lithosphere.

The theoretical geothermal curve (1) has been plotted for the purpose of identifying the distribution of measured heat flow to a theoretical one. It can be seen from Fig. 2 that the right-hand theoretical geothermal curve is a sufficiently good fit to the maximum measured heat flow values, indicating the early Miocene as the time when the Kamchatka Basin began to form (anomaly 6A, 21 Ma).

It thus appears that the opening of the Kamchatka Basin began in the Early Miocene, as follows from this analysis of geothermal and geomagnetic data. The spreading in the northern part of the basin (north of the Alpha Fracture Zone) began ~16 Ma (Middle Miocene) as estimated from heat flow data. An analysis of banded magnetic anomalies north of the Commander Islands (anomalies 5C, 5D, 6, 6A) indicates a pattern of increasingly younger anomalies in the northeast direction (the oldest anomaly 6A is situated at the southernmost end of the basin) and a regularly decreasing distance between anomalies of the same name in that direction [3]. This provides evidence for "propagation," that is, a gradual northeastward advance of the spreading in the Kamchatka Basin. The heat flow data do not contradict this inference. The stresses produced at the contact of the Eurasian plate and the Pacific plate, as the latter was being subducted together with the Emperor Seamount structures in the Aleutian Trough, facilitated incipient seafloor spreading in the Kamchatka Basin [9].

The north–south Shirshov Ridge extends for 750 km southward from the Olyutorskii Peninsula to Bowers Ridge. The sedimentary cover of the Shirshov Ridge is thin, viz., 1 km on average. The northern part of the ridge is characterized by moderate heat flow values, 51–68 mW/m^2, while values as high as 77–87 mW/m^2 were measured in the southern part of the ridge, near its junction with Bowers Ridge (Fig. 2). This shows that the ridge formed in a series of episodes.

We estimated the age of the northern and southern Shirshov Ridge from the geothermal relation (2) for structures of nonoceanic origin [5]:

$$t = e^{4.54[(\ln 480 - 1) - \ln q]} = e^{(23.49 - 4.54 \ln q)}, \qquad (2)$$

where t is the age of the structures in Ma and q the heat flow in mW/m^2.

From (2) it follows that the northern part of the ridge has an age of 95 Ma (Late Cretaceous) based on the background heat flow for that area (65 mW/m^2). This estimate, which is based on heat flow data, is consistent with that based on geological data; the age of cherty rocks dredged up there is the Late Cretaceous [4].

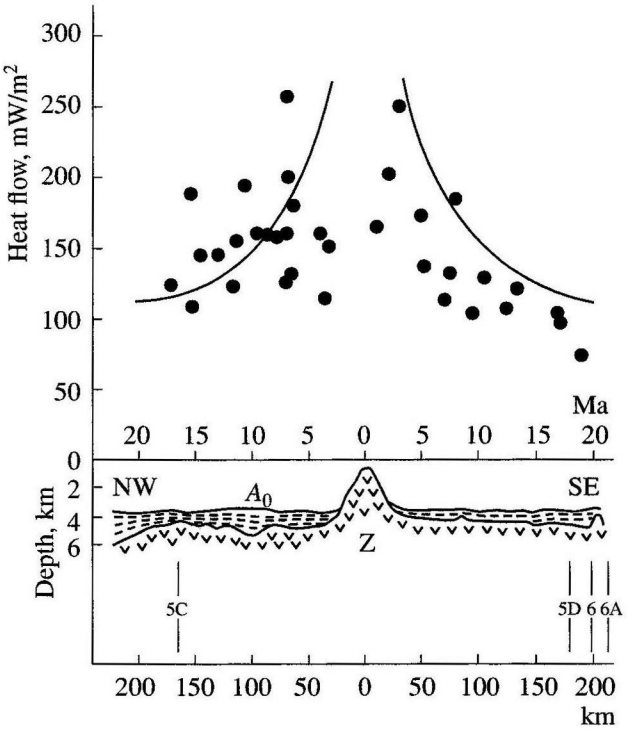


Fig. 2. Geological–geothermal traverse across the axis of opening (Vulkanologov massif, Commander graben) in the southwestern Kamchatka Basin. Heat flow after [24], magnetic anomalies after [3]. A_0 is seafloor, Z the acoustic basement.

The estimate for the time of origin of the southern Shirshov Ridge based on a background heat flow of 82 mW/m^2 will equal, according to (2), 33 Ma (Early Oligocene). This estimate (Early Oligocene) is corroborated by kinematic data acquired in the Bering Sea region [27]. The different ages of the northern and southern parts of Shirshov Ridge (Late Cretaceous and Early Oligocene, respectively) based on heat flow data correspond to their different geological modes of origin. The northern part is an extension of the Kamchatka terrane structure, while the southern part is composed of island-arc igneous complexes.

The Aleutian Basin is located southeast of the Shirshov Ridge, and extends for 2100 km, as far as the Alaskan coast. The central part of the Aleutian Basin is occupied by the Vitus Rise with sediments ~4 km thick. The magnetic lineations in the area of the rise cannot be reliably identified with the paleomagnetic geochronologic scale [40]. For this reason we estimated the time of origin of the rise from heat flow data.

The background heat flow on Vitus Rise is ~60 mW/m^2. The heat flow from the interior (at the basement top), when corrected for high sedimentation rates during Cenozoic time (50–80 m/Myr, DSDP boreholes 184 and 190), is equal to ~70 mW/m^2. The lithosphere age as estimated from the heat flow 70 mW/m^2 using (1) is

44 Ma [53]. This is consistent with the estimated age for the Aleutian Basin (Early Cenozoic) based on seismostratigraphic and other geological and geophysical data [40].

The background heat flow on Vitus Rise, 60 mW/m^2, is about 20% in excess of that in the northern Aleutian Basin (47 mW/m^2). Judging from the whole body of geophysical evidence, the Aleutian Basin had been underlain by the pre-Cenozoic lithosphere of the Kula plate before spreading began [39]. We think that the low heat flow observed there reflects the geothermal regime of the residual Kula plate fragment [34]. The estimate using (1) for the age of this part of lithosphere in the Aleutian Basin, based on background heat flow values and incorporating the sedimentation corrections (57 mW/m^2), is equal to ~70 Ma (Late Cretaceous). The oldest rocks that have been dredged at the Aleutian island arc are basalt porphyrite (85 Ma) and pyroxene basalt (96 Ma) [4]. The age of the lithospheric fragment in the northern Aleutian Basin as found above from geothermal data (70 Myr) neatly fits into the lifetime of the Kula plate (85–43 Ma) as found from magnetic anomalies [68].

The arcuate Bowers Ridge, which extends for about 900 km from the Aleutian arc to the northwestern end of Shirshov Ridge, is located In the southern Aleutian Basin. The sediment thickness of Bowers Ridge does not exceed 1 km. Near the northeastern part of the ridge is a sediment-filled trench of unknown origin [55].

The average age of Bowers Ridge can be estimated from heat flow data using (2) for structures of nonoceanic origin. From the average heat flow measured on the ridge (84 mW/m^2), its age is ~30 Ma (Late Oligocene). This estimate is consistent with geological evidence, as the terrigenous rocks dredged in the upper part of the Bowers Ridge section are Miocene [4]. This estimate also indicates a similar time of origin for Bowers Ridge and the southern Shirshov Ridge, ~33 Ma (Early Oligocene).

Bowers Ridge separates the Bowers Basin, which is approximately 500 km long, from the Aleutian Basin. The sediments in the basin are thin (1–2 km). The basin contains no well-dated magnetic lineations [4].

We estimated the age of the Bowers Basin using (1) for a geothermal model of seafloor origin by spreading. From (1) it follows that for the background heat flow in the basin (75 mW/m^2) the age of its basement is 40 Ma (Late Eocene). This estimate is confirmed by seismic investigations. An Eocene–Oligocene–Miocene sedimentary sequence was identified in the lower part of the seismic section [4].

The age estimates for the Bering Sea floor features based on heat flow and other geological and geophysical data will be used below in calculations of plate kinematics for the North Pacific.

Numerical Experiments to Model the Thermal Generation of Regional Faults in the Pacific

This paper presents a numerical model that is the first successful attempt at explaining the origin of strike–slip boundaries (regional transform faults as long as 5000 km in the Pacific) as a result of a secondary roller system of convective cells operating in the spreading–subduction system [23]. In this way, the fundamental problem is solved of how the segmentary structure of different spreading axes was formed.

Until recently there has been no explanation of the origin of such long (1000–4000 km or longer) regional features in the North Pacific as the Emperor Fracture Zone, Chinook Trough and other such features. A viable explanation will enable a sound tectonic analysis of the region, optimized calculations for the distribution of isochronous ages for the zone of quiet magnetic field and, consequently, reliable geodynamic reconstructions for the evolution of the lithosphere in various areas of the Pacific.

The explanation offered below for the generation of regional faults in the Pacific seafloor naturally follows from modeling of the global mantle convection in the framework of a thermoconcentration (thermochemical) model [22, 23] incorporating the endothermic phase transition at the boundary between the upper and lower mantle. The numerical modeling showed that the global convection going on at large Rayleigh numbers and with the barrier character of phase transition at 670 km depth has an adjustable mechanism. Lighter material rising from the outer core is completely or almost completely retarded, for a long period, by the phase barrier at the lower–upper mantle boundary. The result is that the lighter component and heat are stored below that boundary. The convection structure is so modified as to overcome the phase barrier at a localized boundary area, where the light material finds its way into the upper mantle. As the stored thermal energy is being exhausted for the endothermic phase transition, the material stops flowing, and the convection in the lower and upper mantle becomes separate again in the region.

The noninertial movement in the upper mantle is modeled in the Boussinesque approximation. The movement at each time instant is then determined by the current density distribution, which is expressed in the thermochemical model, according to the Boussinesque approximation, as follows:

$$\rho = \rho_0(1 - \alpha T - C), \qquad (3)$$

where ρ g/cm^3 is local upper mantle density, ρ_0 = 3.8 g/cm^3 is the average upper mantle density, α deg^{-1} is the coefficient of thermal expansion, T is Kelvin temperature, and C is the dimensionless concentration of lighter material.

The fundamental result derived in the framework of a liquid mantle model is that the divergent boundaries

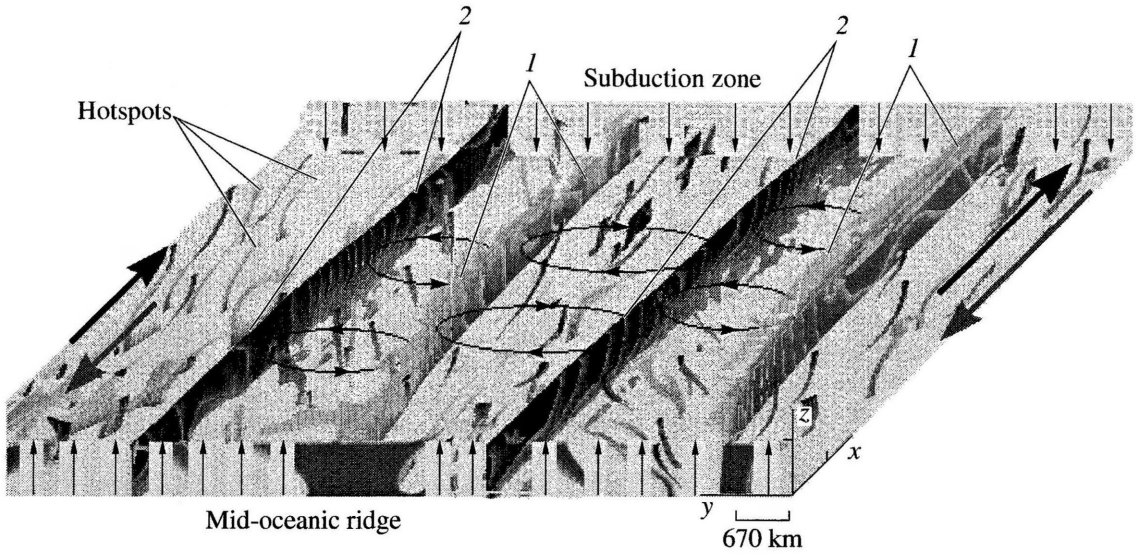


Fig. 3. Cold and hot boundaries of secondary roller flows arising in the upper mantle during forced thermal convection with a Rayleigh number of 10^7. Color shadings show the distribution of temperature inhomogeneities in the numerical experiment. Solid arrows show directions of main flow, thinner lines and arrows indicate directions of secondary flows: (*1*) ascending boundaries of secondary mantle flows (areas of soft lithosphere are transform faults), (2) descending boundaries of secondary mantle flows (areas of rigid lithosphere).

(mid-oceanic ridge zones) and convergent boundaries (subduction zones) between plates on the Earth's surface correspond to boundaries between convective mantle cells below. The third, strike-slip, type of boundary observed on the surface (transform faults) has not been amenable to a simple hydrodynamic treatment.

The first step in this numerical experiment modeling of the generation of regional seafloor faults was to simulate forced thermal convection in the upper mantle, in accordance with the well-known theoretical circulation of material between a mid-oceanic ridge and a subduction zone located parallel to one another. This forced upper mantle circulation is usually attributed to a nonuniform heating on the part of the upper mantle. This scheme implies a quasi-stationary, long-continued, separate two-depth convection going on in the complete mantle involving identical rotation of the material in the upper and lower mantle. We note that the material at the boundary is moving in opposite directions.

The region to be modeled is a parallelepiped with two horizontal (longitudinal x and transverse y) coordinates and one vertical z (Fig. 3). The transverse or end faces of the region were used to simulate a mid-oceanic ridge and a subduction zone, where mirror symmetry about the ridge was required to hold. The longitudinal lateral faces were chosen to be sufficiently far from each other, and we assigned "soft" conditions there to ensure the periodicity of the solution along the transverse coordinate y. The temperature is constant (low) at the top face of the region, there are no vertical velocity and tangential stresses. At the bottom a (high) temperature was assigned that was linearly and slowly increasing along the longitudinal coordinate x from the subduction face to the mid-oceanic face, the velocity of mantle flow being set equal to zero.

The first, auxiliary, purpose of these numerical experiments was to obtain the main flow—forced thermal convection in the form of an elongate circulation of material in the longitudinal direction—from the subduction zone to the mid-oceanic ridge. It turned out that 5–10% of the longitudinal temperature gradient was sufficient to give rise to the expected main circulation flow, no matter what the initial temperature distribution within the region was.

The main goal of our numerical experiments was to investigate secondary flows, conditions for their generation, and spatial structure. Calculations showed that at Rayleigh numbers on the order of 10^6 secondary flows in the form of roller convection in the transverse direction begin to appear, while at Rayleigh numbers equal to 10^7 the secondary roller flows are mature and show well-defined straight boundaries (Fig. 3). These boundaries have two alternating (in space) types, namely, cold boundaries, involving a downward movement of mantle material, and hot boundaries, involving an ascending movement. Evidently, it is only the hot ascending boundaries of secondary convective cells, which produce tension in the mantle, that should be associated with transform faults, while the cold boundaries play the opposite role of a kind of rigid reinforcement member that holds together the longitudinal pieces resulting from the upper mantle being cut by the hot convective boundaries.

Another feature observed in the experiments [21] consists in thin thread-like structures (plumes), which are sharply prominent against the surrounding background in temperature, and divide into two types, ascending hot, and descending cold, jets. The thread-like structures forming at large Rayleigh numbers occur in space and time chaotically, but are moving and assume inclined curved shapes exactly as required by the spiral character of movement around them described above. The hot thread-like structures provide a natural explanation of the hotspots observed on the surface of our planet (Fig. 3).

The viscous liquid model is certainly a crude approximation of the actual terrestrial mantle, which consists of a solid elasticoplastic material, but this model provides an essential understanding of the origin of the most significant seafloor features, which obey the laws of the dynamics of continua.

This modeling of the generation of regional transform faults confirms the inferences drawn from an analysis of tectonic evidence [8], viz., that the origin of such faults cannot possibly be related to spreading (e.g., the Emperor Fracture Zone, Chinook Trough and others). This makes it possible to optimize our technique for calculating isochronous seafloor ages for the zone of quiet magnetic field, hence of developing plate tectonic reconstructions for the evolution of the North Pacific.

As mentioned above, plate tectonic reconstructions require knowledge of isochronous seafloor ages in the North Pacific. This primarily concerns the region of quiet magnetic field. Some of the longer trough features in the North Pacific (Mendocino, Emperor, Chinook) are situated in the zone of quiet magnetic field. It is for this reason that one frequently encounters contradictory models for the origin of such features. This fully applies to the Emperor Trough, which is believed [60, 61] to have been an older spreading center. However, in the light of the above model, the Emperor Trough is a regional transform fault, which is well borne out by a detailed analysis of tectonic data around this feature [8]. This fact was the basis of our calculations of isochronous seafloor age for the North Pacific, which we have used to develop the four plate tectonic reconstructions for the North Pacific presented here.

THE GEODYNAMICS OF THE NORTH PACIFIC

One of the most important parameters in plate tectonic reconstructions is the age of seafloor features, as found from combined geological and geophysical data, in the first place from datings of dredged and drilled rocks, as well as from magnetic and heat flow measurements.

Apart from the North Pacific (north of Hawaii), the area of study also includes the Bering Sea. The age of the open part of the North Pacific seafloor is determined from magnetic lineations and by age interpolations between magnetic anomalies in the zone of quiet magnetic field [8, 37, 54, 61]. In addition, a reliable interpretation of seafloor age distributions in this part of the Pacific requires a clear understanding of the origin of the major extended features existing there. It was mentioned above that the origin of such features can be treated in two alternative ways, either as transform faults or as older spreading axes. The modeling carried out in this study confirmed a faulting (not a spreading) origin of such features as the Emperor Fracture Zone, Chinook Trough [8] and others.

According to the geological history of the North Pacific, the controlling parameters for geodynamic calculations are the age values for Bering Sea features, because the Bering Sea region had belonged to the Pacific Ocean floor (Kula plate) prior to the generation of the Aleutian arc during early Tertiary time [15, 39].

The Bering Sea includes extensive continental shelves of North America and Eurasia, as well as the deep-sea Aleutian, Bowers, and Kamchatka basins (Fig. 1). The main features that separate these basins are the Shirshov and Bowers ridges. Deep drilling in the Bering Sea (wells DSDP 188–191) reached the basement in the Kamchatka Basin only (well 191) [44], the other wells penetrating Miocene and younger deposits in the sediments [64]. As well, magnetic anomalies have been dated on the paleomagnetic stratigraphic scale for the Kamchatka Basin only.

Overall, reliable data on the age of seafloor features in the Bering Sea are not available. For this reason, special importance will attach to our estimates of the ages of features based on heat flow measurements, as well as on dredging and other indirect evidence relating to the geological structure of the Bering Sea continental circumference.

The Bowers Ridge is arcuate with the convex side northward, toward the Aleutian Basin; it intervenes between this basin and Bowers Basin. The ridge has no recent seismicity and is asymmetric in structure, dipping at a lower angle to the north than to the south. A trench filled with 9–10 km sediment is adjacent to the ridge from the north, where the Aleutian Basin is situated [41]. Well DSDP 188 penetrated only Miocene and younger sediments in the southern flank of the ridge [42]. Occasional dredging on the ridge brought up a few samples of altered volcanic rocks and diorites of undetermined age. These rocks are similar to those found at the base of the Aleutian island arc [63]. The structural setting and shape of the ridge, the presence of a trench, as well as the magnetic lineation pattern above the ridge [55], are all pieces of evidence that combine to suggest that the Bowers Ridge is an older island arc with an older Zavaritsky–Benioff zone dipping south. While there is a consensus among researchers about the origin of the ridge, contradictory opinions exist as to its age interpretation. Some researchers believe the ridge to be

an early Tertiary branching of the Aleutian island arc [63], others think it is a Mesozoic island arc [59], and still others suggest it is a remnant of the island arc transported by the Kula plate from the south [36]. We determined the age of the Bowers Ridge as Oligocene time (30 Ma) from heat flow data, indicating an early Tertiary origin.

The Bowers Basin is small, and is situated between Bowers Ridge and the Aleutian arc. It is behind Bowers Ridge, which has a well-defined arcuate shape, and is evidently a backarc basin. There are undated, nearly north–south, magnetic lineations identified in the basin [41]. We determined the age of the basin seafloor as 40 Ma (Eocene) from geothermal data. This figure is in sufficiently good agreement with the estimated age of Bowers Ridge (30 Ma) and corroborates the origin of the basin as a result of backarc spreading.

Shirshov Ridge extends from the Olyutorskii Peninsula of Kamchatka for about 700 km nearly due south. It can safely be asserted that the southern part of the Shirshov Ridge has an extension onto the Bowers Ridge. This fact is not very well expressed morphologically, but the relationship is clearly perceived in maps of basement features, and in maps of magnetic and gravity (free air) fields [40]. The Shirshov and Bowers ridges are adjacent in a sinistral offset of nearly 350 km. The Shirshov Ridge is 2–2.5 km high and has an asymmetrical structure. The east slope dips gently east and is overlain by gently dipping sediments that can be followed without interruption into the Aleutian Basin [26]. This shows that the ridge basement was connected with the basalt floor of the Aleutian Basin prior to the deposition of its sedimentary cover. Because deep sea drilling (well DSDP 190) did not reach the basement [43], but only penetrated Miocene deposits, there is no reliable evidence for the age of the sediment bottom in the Aleutian Basin. Consequently, it has not been determined when Shirshov Ridge became connected with the basalt basement of the Aleutian Basin. The west side of the ridge is dipping stepwise west toward the Kamchatka Basin in a series of high-angle listric scarps [26]. The normal listric faults formed in the western flank of Shirshov Ridge in relation with the extension, rifting, and spreading in the Kamchatka Basin during the past 25 Myr; this did not take place until after the complex imbricated thrust structure formed in the northern part of the ridge as a result of collision with the subduction boundary of Eurasia in the Karyakia area at approximately 40 Ma.

There is a wide gamut of opinion as to the origin of Shirshov Ridge. It has been considered as an aseismic volcanic ridge, a hotspot track [36], an assemblage of tectonic sheets in a thickened oceanic crust [26], a foreign block (terrane) [15], or as an island-arc block [27].

It should be said, more accurately, that the Shirshov Ridge evidently has a more complex structure than has been thought previously. The northern part of the ridge is a southward underwater extension of the Kamchatka terrane structure. Very diverse rocks have been dredged in this zone [1], the most frequent ones including gabbro and amphibolites, as well as cherty rocks of a wide range of ages (Radiolaria found there indicate the presence of Middle and Upper Triassic, Upper Cretaceous and Paleogene, Oligocene, and Miocene ages). In addition, numerous volcanic island arc rocks have been dredged [2]. The whole of these findings thus indicates that the northern part of the ridge is composed of deformed and partly metamorphosed rocks (amphibolites) of Mesozoic and Paleogene–Neogene time. All this is reminiscent of the structure of foreign complexes (terranes) in Kamchatka, consisting of an accumulation of tectonic sheets of various origins.

The northern part of Shirshov Ridge has a thrust, imbricated structure as well. Island-arc igneous rocks (andesites) have been dredged in the southern part of the ridge; their absolute age was found to be 16.8 Ma [63]. This part extends into the western part of Bowers Ridge, judging from geomagnetic and gravity data [40].

The conclusion reached here as to differences in the geological structure between the northern and southern parts of Shirshov Ridge is corroborated by geothermal data. The average age of the lithosphere based on heat flow measurements is 95 Ma (Upper Cretaceous) for the northern part and 33 Ma (Oligocene) for the southern portion. The latter estimate is very close to the Oligocene age found for Bowers Ridge from heat flow data, ~30 Ma.

Summing up the above arguments, we consider Shirshov Ridge as a complex Upper Cretaceous terrane (possibly as a structural extension of the Olyutorskii zone) on which (at least on some part of it) an island arc formed later that was operating simultaneously with the Bowers Ridge arc. The two arcs seem formerly to have been a single feature, but the Shirshov arc was the more stable, while the Bowers arc was the more mobile. It was the Bowers arc that was experiencing a sinistral offset nearly east–west relative to Shirshov Ridge.

Considering the whole set of geological and geophysical data [1, 2, 40] and the age of Bowers–Shirshov ridges based on geothermal data, we hypothesize the this single Bowers–Shirshov arc formed at about the same time as the Aleutian arc did, and had been active approximately until 30 Ma.

The Kamchatka Basin is situated between Shirshov Ridge and Kamchatka, and is bounded by the Aleutian arc on the south (Fig. 1). The sediments in the basin are thin (1–2 km) [39], so the basin must be young. Well DSDP 191 was drilled there and found MOR basalts (largely altered) in the sediment basement dated as 31 Ma by the K–Ar method [44]. However, that age was subsequently revised to diminish it to ~10 Ma owing to losses in Ar in basalt metasomatism [W. Har-

bert, personal communication, 1986], which is fairly consistent with higher (compared with that for the Aleutian Basin) heat flow (~150 mW/m^2) in the DSDP well area. The sediment column in the well is of Upper Miocene to Pliocene and Upper Pliocene to Holocene age [64]. Magnetic lineations have been identified in the basin [3]. According to the age estimate based on heat flow measurements, the oldest seafloor age in the Kamchatka Basin is 21 Ma. This estimate is fairly consistent with the time the seafloor began to form there, as inferred from magnetic data (anomalies 6, 6A, 5D [3]) (see below). The orientation of the magnetic lineations indicates the spreading direction. The spreading axis was subparallel to the basin sides and across the Commander Islands chain. In that case, the opening of the basin producing a new oceanic crust must inevitably have led to subduction beneath Kamchatka. Young Neogene–Quaternary calc–alkali volcanism has been recorded at the north coast of Kamchatka [17], which confirms this possibility.

To sum up, the spreading in the Kamchatka Basin began approximately 21 Ma by "cleaving off" the west edge of Shirshov Ridge. The active spreading phase terminated approximately 10 Ma, as inferred from magnetic data [3], but is still going on in the southern part of the basin [27].

The Aleutian Basin is covered with sediments 4–5 km thick, which are still thicker (up to 7–9 km) near the continental slope. Magnetic lineations trending north–south were mapped in the basin, but their age remained undetermined; their geometry and extent are typical of spreading anomalies [39, 40]. As pointed out above, the magnetic anomalies recorded there cannot be reliably fitted into the paleomagnetic time scale. Apart from anomalies having the north–south orientation identified in most previous studies, curved and linear anomalies have been detected between the Bowers and Shirshov ridges, traversing the Aleutian Basin north-northeast. The anomalies are related to Vitus Rise, an identifiable basement feature thought to have been due to backarc spreading during Eocene time [40]. We emphasize that the recent interpretations of paleomagnetic ages and the mode of origin for the Aleutian Basin are very uncertain. For example, the basin anomalies were at first identified as anomalies of the Mesozoic sequence M0–M13 (121–136 Ma), while the basin floor was supposed to be part of the Kula plate separated from it by the incipient generation of the Aleutian arc [39]. However, later studies gave a broader time range, Late Cretaceous to Paleogene, for the age of the basin floor [40].

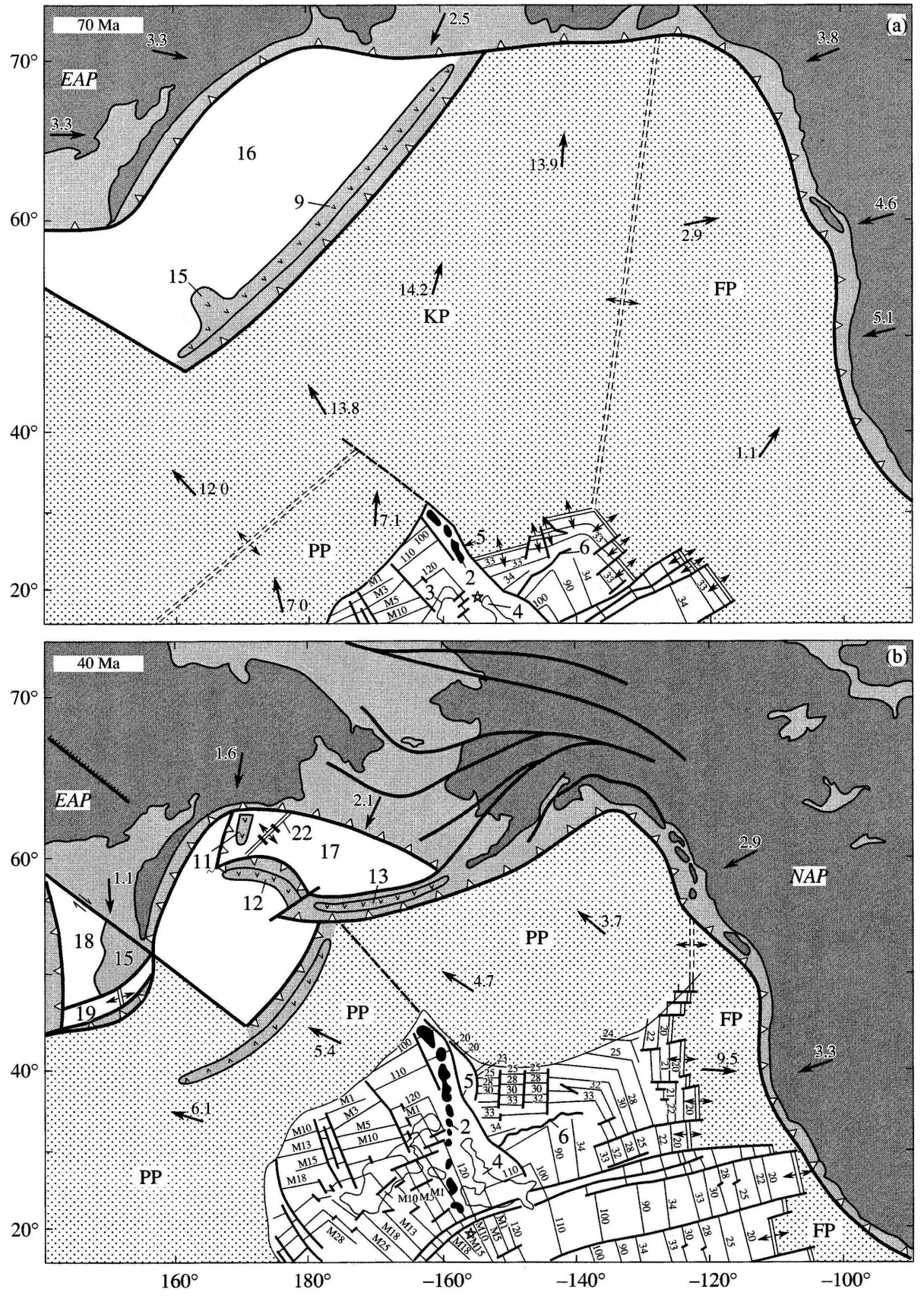
According to our estimate based on heat flow data, the seafloor in the northwestern Aleutian Basin, which has not been involved in backarc processes, has an average age of 70 Ma (Senonian, Upper Cretaceous). This figure is thus in good agreement with the time of existence of the Kula plate (85 to 43 Ma), so that the Aleutian Basin can well be regarded as an outlier of that plate. The age of Vitus Rise is found from geothermal data as 44 Ma (Eocene), corroborating the timing of a regional lithosphere heating there [53]. That backarc spreading event (44 Ma) was simultaneous with a phase of activity at the Bowers island arc and was probably related to the consumption of oceanic crust beneath the Shirshov Ridge arc as well, with the subduction zone dipping toward the Aleutian Basin.

Plate tectonic reconstructions require knowledge of plate boundaries and of how they were changing over time and space, as well as of plate motion parameters. The current plate motion data show three great plates to be interacting in this region, viz., the Pacific, the Eurasian, and North American [45, 69].

The Pacific plate is plunging beneath the Aleutian–Kuril–Kamchatka subduction zone nearly exactly across the Kamchatka trench (azimuth 315° near Kamchatka); this gives the result that the Pacific plate is experiencing pure strike–slip motion (no subduction) relative to the North American plate in the westernmost Aleutian arc, around the Commander Islands.

In the north the Aleutian arc is a boundary to the Pacific plate and has been such a boundary for a long time, at least during the last 55–60 Myr, judging from the age of volcanic rocks found in the Aleutian Islands [66]. It thus appears that until that time, the Bering Sea region had been completely connected with the Pacific deep-sea basins, and thus had a common geological history with the Pacific.

Fig. 4. Plate tectonic reconstructions for the North Pacific in the absolute coordinates (hotspot system) for 70 (a), 40 (b), 33 (c), and 21 (d) Ma: (*1*) areas of continental crust: (a) land, (b) shelf and continental slope; (*2*) areas of oceanic crust, (*3*) consumed (by present) oceanic crust of the following plates: Eurasian (EAP), North American (NAP), Juan de Fuca (JP), Vancouver (VP), Kula (KP), Pacific (PP), Farallon (FP); (*4*) subduction zones, (*5*) spreading zones: (*a*) certain, (*b*) hypothetical; (*6*) zones of collision and overthrusting, (*7*) grabens and normal fault zones, (*8*) strike–slip faults (with indication of displacement where known), (*9*) magnetic lineations and their numbers, as well as seafloor isochrones at 90, 100, 110, and 120 Ma and their ages (*a*), transform faults (inferred extensions of faults are shown by dashed lines) (*b*); (*10*) oceanic island arcs: (*a*) active, (*b*) dead, (*11*) vectors of absolute plate motion relative the hotspot system (cm/yr), not to scale, (*12*) present position of Loihi Seamount as the beginning of Hawaiian–Emperor seamount chain. Ridges: (1) Hawaiian, (2) Emperor; rises: (3) Shatsky, (4) Hess; (5) Emperor Fracture Zone, (6) Chinook Trough; linear seamount chains: (7) Kodiak–Bouvet, (8) Parker–Scott; island arcs (in part based on [5]): (9) Shirshov–Nemuro, (10) Kuril, (11) Shirshov, (12) Bowers Ridge, (13) Aleutian, (14) East Kamchatka peninsulas–Nemuro; (15) central Sea-of-Okhotsk massif; basins: (16) Irune, (17) Aleutian, (18) Deryugin, (19) South Kuril, (20) Bowers, (21) Kamchatka Basin, (22) Vitus Rise.


70 Ma
(a)
EAP
16
9
15
KP
FP
PP
2.5
3.3
3.3
3.8
13.9
4.6
2.9
14.2
5.1
13.8
1.1
12.0
7.1
7.0
70°
60°
40°
20°
40 Ma
(b)
EAP
NAP
PP
FP
1.6
2.1
2.9
1.1
3.7
4.7
5.4
9.5
3.3
6.1
160°
180°
–160°
–140°
–120°
–100°

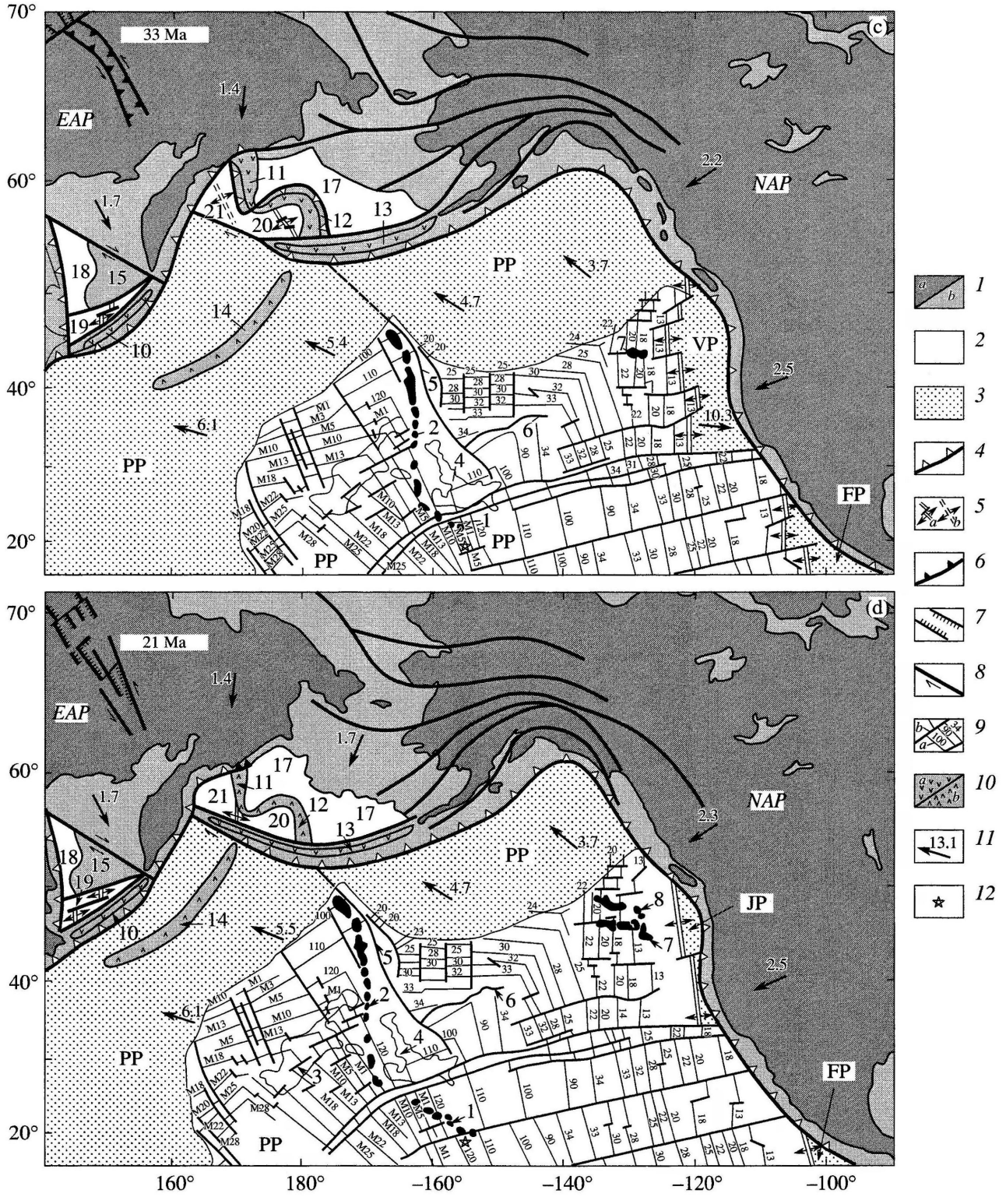


Fig. 4. (Contd.).

The boundary between the North American and Eurasian plates is along Gakkel Ridge in the Arctic Ocean, and can be followed farther by a set of grabens and major strike slip faults exhibiting dispersed seismicity and present-day volcanic activity from the Lena R. mouth into the Laptev Sea through the Omoloi graben and the Mom Rift grabens, as well as the Chersky Range grabens (the Nenneli, Mom–Selennyakh,

Verkhnenera, and Seimchan grabens) nearly as far as Shelikhov Bay in the Sea-of-Okhotsk coast [16]. This boundary seems to have existed in some form or other during the last 50–60 Myr, since Gakkel Ridge formed in the Arctic.

A more detailed examination of the dispersed seismicity along the Bering Sea coasts identifies the Bering Sea plate (or Beringia) within the North American plate [70], in a similar manner to the way the Sea-of-Okhotsk and Amur plates can be identified within the Eurasian plate [69]. The seismicity distribution is to some extent a reflection of the situation that had existed in the Bering Sea region after the birth of the Aleutian island arc. At that time the bulk of seafloor subduction (the Kula and Pacific plates) was assumed by the young Aleutian subduction zone, but the seafloor area that separated from the Pacific Ocean continued to be subducted under the continents around the Bering Sea. As to the west of the region, the subduction in the Kamchatka Basin area under the Kamchatka region of Eurasia continued until ~10 Ma.

The history of the region, accompanied with suitable paleogeodynamic constructions, has been examined by many researchers, the most significant contributions being [13, 15, 20, 25, 27, 33, 35, 40, 41, 66, 67]. Because of lack of space we do not discuss details in the geological evolution of the region, such as the Late Cenozoic migration of the Kamchatka volcanic zones, the morphologic and neotectonic differences between the Kuril–Kamchatka island arc and the Petropavlovsk–Malki transverse dislocation zone and so on, but refer the reader to [11, 18, 27, 32].

The goal of the present study is to show how heat flow data (since geological data are necessarily limited in aqueous areas can be effectively used to date the geological age of seafloor features of different origins [6] and to construct reliable maps of geodynamic evolution for the Bering Sea region on this basis.

We present the geological history of the region in a series of plate tectonic reconstructions for the times 70, 40, 33, and 21 Ma derived from the heat flow data above (Fig. 4). These reconstructions were calculated in absolute coordinates (in the hotspot system). Our calculations of motion for the Pacific plate and other oceanic plates (Kula, Farallon, Vancouver) used data from [19, 46, 47, 56]. The relative motions of the continental Eurasian and North American plates were calculated after [49, 51] and then converted into the absolute hotspot system based on [52, 57]. Investigations showed that the hotspots themselves are slowly moving relative to one another [19]. For the Pacific this motion becomes significant for ages older than 43 Ma. A latitude based on the hotspots should be corrected [19] in order to find the reconstructed paleomagnetic latitude for any point in the Pacific (this does not concern the continental circumference of the Pacific). For a reconstruction for 70 Ma (Fig. 4a), the correction is –11°, that is, 11° is to be subtracted from the latitude of any point in the Pacific Ocean floor.

The absolute motion vectors plotted here demonstrate that the overall motion of the continental Eurasian and North American plates has been oceanward during the last 70 Myr, toward the oceanic plates of the North Pacific that are diverging from one another landward; these are the Pacific, Kula, and Farallon (Vancouver and Juan de Fuca). The smaller plates (e.g., those of marginal seas) obeyed this dominant trend. The translational motion of oceanic plates toward their continental circumference was constantly reproducing a situation of almost continual generation, existence, and subsequent decay of calc–alkali volcanic belts related to subduction zones.

70 Ma (Maastrichtian, Late Cretaceous, Fig. 4a). The reconstruction shows the situation before part of the oceanic Kula plate was separated by the incipient Aleutian subduction zone. At that time the Kula plate was moving nearly due north at a speed of about 14 cm/yr, while the Eurasian plate was moving south at 2–3 cm/yr, that is, the relative convergence rate was about 17 cm/yr. By that time the Sea-of-Okhotsk–Chukchi volcanic belt had almost decayed in activity, and a new subduction zone was forming in the future continental-margin Paleocene–Eocene Anadyr'–Bristol volcanic belt. Simultaneously with this, an extended doubled island arc was operating, which consisted of the following fragments: Nemuro–Minor Kurils–Vityaz Ridge–Sea-of-Okhotsk–East Kamchatka peninsulas (the double to the parallel Osemovo–Valaginskii arc)–Olyutorskii–Bowers Ridge–Shirshov Ridge, with the Benioff zone dipping landward. The island arc separated the extensive Irune Basin from the open ocean.

Our reconstruction shows an extension of the Emperor Fracture Zone along the north side of Obruchev Rise situated at the northwestern termination of Emperor Seamount Chain in the junction area between the Kamchatka and Kuril trenches. In our opinion, the northern extension of Emperor Fracture Zone is part of the Mamua, Kruzenshtern, and Stalemate transform fault system and has the same orientation as these faults, with the northernmost part of Emperor chain coinciding with the northwestward extension of Emperor Fracture Zone. This part of Emperor Fracture Zone was "healed" by volcanic material of Obruchev Rise as it was passing above the Hawaiian hotspot. The situation is analogous to the generation of the Faeroe–Greenland Ridge in the Iceland Fracture Zone [62]. Detailed seismic investigations [65] point to the presence of major depressions in the basement of Obruchev Rise trending along the northeast slope. We think that the depressions mark the near-surface part of Emperor Fracture Zone.

40 Ma (Eocene, Fig. 4b). By the Eocene most of the Aleutian arc had been formed; the arc had cut out a part of the Kula seafloor that would exist in the future as the Aleutian Basin, with the Kula plate itself ceasing to exist. The Pacific plate, which mostly interacted with continental plates in the beginning, changed its direction of motion from northward to northwestward. The Bowers Ridge arc began to operate, and the eponymous backarc basin was formed. The Shirshov Ridge had approached the subduction zone and began to block it. An incipient subduction zone formed beneath the western edge of the ridge, and a new island arc began operating. As a result, backarc spreading processes had been active in the Aleutian Basin, producing Vitus Rise. The Nemuro–Minor Kurils-Vityaz–East Kamchatka peninsulas island arc, which was standing in front of Eurasian edge, ceased to be active, it being only its northernmost end (East Kamchatka peninsulas) which continued its volcanic activity, and therefore had a subduction zone dipping seaward. The present-day Sea-of-Okhotsk structure began to form. The Kuril subduction zone and the South Kuril (backarc) basin formed.

33 Ma (Oligocene, Fig. 4c). By the Oligocene the Aleutian island arc had nearly formed, except for its western Commander Is. part. Also, the older Kamchatka Basin had separated from the Pacific plate along a strike–slip boundary. We think that the plate boundary must have a closed outline [14].

An alternative view holds that the Kamchatka Basin began forming as late as the Late Miocene, with the older Kamchatka Basin seafloor being part of the Pacific plate until that time [27].

The subduction beneath the northern margin of Kamchatka and associated island arc magmatism continued until about 10 Ma, owing to spreading in the older Kamchatka Basin.

The Bowers and Shirshov arcs seem to be at the end of the activity, as was backarc spreading in the Bowers Basin, while backarc processes had completely stopped in the Aleutian Basin. The Nemuro–Minor Kurils–Vityaz'–East Kamchatka peninsulas island arc became completely passive and began to converge toward the Kuril–Kamchatka subduction zone. The backarc spreading was terminating in the southern Sea-of-Okhotsk basin.

21 Ma (Early Miocene, Fig. 4d). The Aleutian island arc had completely formed. The Commander Islands seem to have taken their place at the westernmost end of the arc. Also, the Bowers and Shirshov arcs had become completely passive. The west edge of Shirshov Ridge began to be torn off as a result of backarc spreading behind the Commander Islands, in the southern part of the proto-Kamchatka Basin, while the seafloor of the western proto-Kamchatka Basin continued to be consumed beneath the edge of Kamchatka. The Kuril–Kamchatka subduction zone and the Nemuro–Minor Kurils–Vityaz–East Kamchatka peninsulas island arc continued their convergence to collide before the Late Miocene.

CONCLUSIONS

(1) We examined heat flow and other geological and geophysical data for the North Pacific; a map of geothermal and geomagnetic data for the region has been constructed.

(2) Heat flow data were used to derive numerical estimates for the age of the Bering seafloor features: Kamchatka Basin (21 Ma), Shirshov Ridge (95 Ma for its northern part and 33 Ma for the southern), Aleutian Basin (70 Ma), Vitus Rise (44 Ma), Bowers Ridge (30 Ma), and Bowers Basin (40 Ma). These age estimates are corroborated by integrated geophysical and plate-kinematic evidence.

(3) A thermochemical model of global mantle convection was used to carry out numerical modeling of the generation of extended regional features in the North Pacific (the Emperor Fracture Zone, Chinook Trough, etc.). The modeling suggests a plume tectonic origin for these features. With these results in hand, it has been possible to develop the optimal model of tectonic evolution for the North Pacific Ocean.

(4) An analysis is provided for the geodynamic situation in the North Pacific Ocean. It is pointed out that reliable data on the age of various geologic features are not available.

(5) An integrated analysis of geological and geothermal data indicates that the northern Shirshov Ridge is of an imbricated thrust terrane nature, while the southern part of the ridge is of ensimatic island-arc origin similar to that of Bowers Ridge. The Aleutian Basin seafloor is an outlier of the Upper Cretaceous oceanic Kula plate, in which backarc spreading processes originated around Vitus Rise during Eocene time. The terminating phase of activity in the Bering Sea began about 21 Ma with spreading on the older oceanic floor of the Kamchatka Basin.

(6) Age estimates for geologic features in the Bering Sea based on heat flow and on an integrated analysis of magnetic, tectonic, and geological data, together with numerical modeling of thermal processes involved in the generation of extended regional faults, were used to develop plate tectonic reconstructions (in the hotspot system) for the evolution of the North Pacific Ocean relevant to 21, 33, 40, and 70 Ma.

ACKNOWLEDGMENTS

This work was supported by the Russian Foundation for Basic Research, project no. 04-05-64009.

REFERENCES

1. Baranov, B.V., Basov, I.A., and Gladkikh, P.A., Bedrock of the Shirshov Ridge, Bering Sea, *Okeanologiya*, 1984, vol. 24, no. 6, pp. 935–941.
2. Bogdanov, N.A., Vishnevskaya, V.S., and Sukhov, A.N., Upper Cretaceous Formations of the Undersea Shirshov Ridge, Bering Sea, *Dokl. AN SSSR*, 1983, vol. 273, no. 5, pp. 1183–1187.
3. Valyashko, G.M., Chernavskii, G.B., Seliverstov, N.I., et al., Backarc Spreading in the Kamchatka Basin, *Dokl. AN SSSR*, 1993, vol. 338, no. 2, pp. 212–216.
4. Vasil'ev, B.I., Sigova, K.I., Obzhirov, A.I., et al., *Geologiya i neftegazonosnost' okrainnykh morei severo-zapada Tikhogo okeana* (Geology and Gas–Oil Potential of Marginal Seas of Northeast Pacific), Vladivostok: Dal'nauka, 2001.
5. Verzhbitskii, E.V., Geothermal Regime, Seafloor Tectonics, and Temperature Conditions for the Generation of Hydrocarbons in the Eastern Barents Sea, *Geotektonika*, 2002, no. 1, pp. 86–96.
6. Verzhbitskii, E.V., Geothermal Regime and Age of Oceanic and Continental Lithosphere: The Ionic and Adriatic Basins of the Mediterranean, *Okeanologiya*, 2001, vol. 41, no. 1, pp. 132–137.
7. Verzhbitskii, E.V., Zolotarev, V.G., and Sborshchikov, I.M., Heat Flow in Backarc Basins: the Tyrrhenian Sea, *Okeanologiya*, 1991, vol. 312, no. 1, pp. 164–168.
8. Verzhbitskii, E.V. and Kononov, M.V., Heat Flow and Geodynamics of Shatsky and Hess Rises, *Okeanologiya*, 2004, vol. 44, no. 3, pp. 432–439.
9. Verzhbitskii, E.V., Kononov, M.V., Byakov, A.F., et al., The Origin of Hawaiian Ridge and Emperor Seamount Chain, Pacific Ocean, *Dokl. RAN*, 2005, vol. 403, no. 3, pp. 399–404.
10. Galushkin, Yu.I., Murav'ev, A.V., Smirnov, Ya.B., et al., A Study in the Structure of Geothermal Field in the Lithosphere of the Southern Kamchatka Basin, *Vulkanol. Seismol.*, 1986, no. 5, pp. 3–17.
11. Gladenkov, Yu.B., Shantser, A.E., Chelebaeva, A.I., et al., *Nizhnii paleogen zapadnoi Kamchatki (stratigrafiya, paleogeografiya, geologicheskie sobytiya* (The Lower Paleogene of Western Kamchatka: Stratigraphy, Paleogeography, Geological Events), Moscow: GEOS, 1997.
12. Gol'mshtok, A.Ya., On the Influence of Sedimentation on Heat Flow from the Interior, *Okeanologiya*, 1979, vol. 19, no. 6, pp. 1133–1138.
13. Zonenshain, L.P., Kaz'min, V.G., Natapov, L.M., et al., *Paleogeograficheskii atlas Severnoi Evrazii* (A Paleogeographic Atlas of North Eurasia), Moscow: Institut tektoniki litosfernykh plit RAEN, 2000. A compact disk.
14. Zonenshain, L.P. and Savostin, L.A., *Vvedenie v paleogeodinamiku* (An Introduction into Paleogeodynamics), Moscow: Nedra, 1979.
15. Zonenshain, L.P., Kuz'min, M.I., and Natapov, L.M., *Tektonika litosfernykh plit territorii SSSR* (Plate Tectonics of the USSR Area), Book 2, Moscow: Nedra, 1990.
16. Zonenshain, L.P., Natapov, L.M., Savostin, L.A., et al., Plate Tectonics of Northeast Asia in Connection with the Opening of the Arctic Basin and North Atlantic, *Okeanologiya*, 1978, no. 6, pp. 38–47.
17. Kepezhinskas, P.K., *Kainozoiskie vulkanicheskie kompleksy raionov kraevykh morei* (Cenozoic Volcanic Complexes of Marginal Seas), Moscow: Nauka, 1990.
18. Kirmasov, A.B., Solov'ev, A.V., and Khourigan, Dzh.K., Collisional and Postcollisional Structural Evolution of the Andrianov Suture (Sredinnyi Range, Kamchatka), *Geotektonika*, 2004, no. 4, pp. 64–90.
19. Kononov, M.V., *Tektonika plit severo-zapada Tikhogo okeana* (Plate Tectonics of Northwest Pacific Ocean), Moscow: Nauka, 1989.
20. Konstantinovskaya, E.A., The Mechanism of Continental Crustal Accretion: Western Kamchatka, *Geotektonika*, 2002, no. 5, pp. 59–78.
21. Kotelkin, V.D., Some Features of Mature Thermal Convection and their Geophysical Effects, in *Sovremennye problemy aerogidrodinamiki. Tez. dokladov XI shkoly-seminara* (Contemporary Problems of Aerohydrodynamics. Abstracts of papers, XI School–Seminar), MGU, 2003, pp. 47–48.
22. Lobkovskii, L.I. and Kotelkin, V.D., A Two-stage Thermochemical Model for Mantle Convection and its Geodynamic Corollaries, in *Problemy global'noi geodinamiki: Mater. Teoreticheskogo seminara OGGGGN RAN, 1998–1999* (Problems of Global Geodynamics. Materials of OGGGGN RAN Theoretical Seminar, 1998–1999), Rundkvist, D.V., Ed., Moscow: GEOS, 2000, pp. 29–53.
23. Lobkovskii, L.I. and Kotelkin, V.D., An Alternating Thermoeclogite Convection in the Mantle Incorporating the Phase Transition at 670 km Depth, a Comparison with Seismic Tomography Data, in *Tektonika neogeya: obshchie i regional'nye aspekty. Mater. XXXIV Tektonicheskogo soveshchaniya* (Neogene Tectonics: General and Regional Aspects. Materials of the XXXIV Tectonic Conference), Moscow: GEOS, 2001, vol. 1, pp. 378–381.
24. Murav'ev, A.V., The Geothermal Field of Backarc Basins: Bering and Philippine Seas, Cand. Sci. Dissertation, Moscow: GIN, 1990, p. 45.
25. Nekrasov, G.E., The Tectonic Nature of the Koryak–Kamchatka Region and the Geodynamics of the Pacific Northwest Folded Circumference, *Geotektonika*, 2003, no. 6, pp. 53–79.
26. Neprochnov, Yu.P., Sedov, V.V., and Merklin, L.P., The Tectonic Structure of Shirshov Ridge, Bering Sea, *Geotektonika*, 1985, no. 3, pp. 21–37.
27. Seliverstov, N.I., *Stroenie dna prikamchatskikh akvatorii i geodinamika zony sochleneniya Kurilo-Kamchatskoi i Aleutskoi ostrovnykh dug* (Seafloor Structure of Water Areas off Kamchatka and the Geodynamics of the Junction Zone between the Kuril–Kamchatka and Aleutian Island Arcs), Moscow: Nauchnyi Mir, 1998.
28. Smirnov, Ya.B., Sugrobov, V.M., and Galushkin, Yu.I., Heat Flow in the Junction Zone between the Kuril–Kamchatka and Aleutian Island Arcs, *Vulkanol. Seismol.*, 1982, no. 6, pp. 96–115.
29. Smirnov, Ya.B. and Sugrobov, V.M., Terrestrial Heat Flow in the Kuril–Kamchatka and Aleutian Provinces. 2. A Map of Measured and Background Heat Flows, *Vulkanol. Seismol.*, 1980, no. 1, pp. 16–31.
30. Smirnov, Ya.B. and Sugrobov, V.M., Terrestrial Heat Flow in the Kuril–Kamchatka and Aleutian Provinces. 3.

Estimate of Temperature at Depth and Lithosphere Thickness, *Vulkanol. Seismol.*, 1980, no. 2, pp. 3–18.

31. Smirnov, Ya.B. and Sugrobov, V.M., Terrestrial Heat Flow in the Kuril–Kamchatka and Aleutian Provinces. 1. Heat Flow and Tectonics, *Vulkanol. Seismol.*, 1979, no. 1, pp. 59–73.
32. Solov'ev, A.V., Brendon, M.T., Garver, Dzh.I., and Shapiro, M.N., The Kinematics of the Vatyn–Lesnovskii Overthrust, Southern Koryakia, *Geotektonika,* 2001, no. 6, pp. 56–74.
33. Stavskii, A.P., Chekhovich, V.D., Kononov, M.V., et al., Plate Tectonics and Palinspastic Reconstructions for the Anadyr'–Koryak Region, *Geotektonika*, 1988, no. 6, pp. 32–42.
34. Khain, V.E., *Tektonika kontinentov i okeanov (god 2000)* (The Tectonics of Plates and Continents: The Year 2000), Moscow: Nauchnyi Mir, 2001.
35. Chekhovich, V.D., Bogdanov, N.A., Kravchenko-Berezhnoi, I.R., et al., *Geologiya zapadnoi chasti Beringovomor'ya* (The Geology of the Western Bering Sea), Moscow: Nauka, 1990.
36. Ben-Avraham, B.Z. and Cooper, A.K., Early Evolution of the Bering Sea by Collision of Oceanic Rises and North Pacific Sunduction Zones, *Geol. Soc. Amer. Bull.*, 1981, vol. 92, pp. 485–495.
37. Cande, S.C., Larson, R.L., Pitman, W.C., et al., *Magnetic Lineation Map of the World*, Palisades–New York: Lamont-Doherty Geol. Observatory, 1986.
38. Carlson, R.L. and Johnson, H.P., On Modeling the Thermal Evolution of the Oceanic Upper Mantle: An Assessment of Cooling Plate Model, *J. Geophys. Res.*, 1994, vol. 99, no. B2, pp. 3201–3214.
39. Cooper, A.K., Marlow, M.S., and Scholl, D.W., Mesozoic Magnetic Lineations in the Bering Sea Marginal Basin, *J. Geophys. Res.*, 1976, vol. 81, pp. 1916–1934.
40. Cooper, A.K., Marlow, M.S., Scholl, D.W., and Stevenson, A.J., Evidence for Cenozoic Crustal Extension in the Bering Sea Region, *Tectonics*, 1992, vol. 11, no. 4, pp. 719–731.
41. Cooper, A.K., Scholl, D.W., and Marlow, M.S., Structural Framework, Sedimentary Sequences, and Hydrocarbon Potential of the Aleutian and Bowers Basins, Bering Sea, in *Geology and Resource Potential of the Continental Margin of Western North America and Adjacent Ocean Basin—Beaufort Sea to Baja California, Earth Sci. Ser.*, 1987, vol. 6, pp. 473–502.
42. Creager, J.S., Scholl, D.W., Boyce, R.E., et al., Site 1888, *Initial Rep. Deep Sea Drill. Proj.*, 1973, vol. 19, pp. 263–305.
43. Creager, J.S., Scholl, D.W., Boyce, R.E., et al., Site 190, *Initial Rep. Deep Sea Drill. Proj.*, 1973, vol. 19, pp. 359–412.
44. Creager, J.S., Scholl, D.W., Boyce, R.E., et al., Site 191, *Initial Rep. Deep Sea Drill. Proj.*, 1973, vol. 19, pp. 314–367.
45. De Mets, C., Gordon, R.G., Argus, D.F., and Stein, S., Current Plate Motions, *Geophys. J. Int.*, 1990, vol. 101, no. 2, pp. 425–478.
46. Engebretson, D.C., Cox, A., and Gordon, R.G., Relative Motions between Oceanic Plates of the Pacific Basin, *J. Geophys. Res.*, 1984, vol. 89, no. 12, pp. 10291–10310.
47. Engebretson, D.C., Cox, A., and Gordon, R.G., *Relative Motions between Oceanic and Continental Plates in the Pacific Basin, Bull. Geol. Soc. Amer. Spec. Pap.*, 1985, vol. 206.
48. Farrar, E. and Dixon, J.M., Early Tertiary Rupture of the Pacific Plate: 1700 km of Dextral Offset along the Emperor Trough–Line Islands Lineament, *Earth Planet. Sci. Lett.*, 1981, vol. 53, no. 3, pp. 307–323.
49. Gaina, C., Roest, Muller, R.D., Late Cretaceous–Cenozoic Deformation of Northeast Asia, *Earth Planet. Sci. Lett.*, 2002, vol. 197, pp. 273–286.
50. Gordon, R.G., Paleomagnetic Test of the Emperor Fracture Zone Hypothesis, *Geophys. Res. Lett.*, 1982, vol. 9, no. 11, pp. 1283–1286.
51. Klitgord, K.D. and Schouten, H., Plate Kinematics of the Central Atlantic, in *The Geology of North America. V. M. The Western North Atlantic Region*, Vogt, P.R. and Tucholke, B.E., Eds., Boulder, Co.: Geol. Soc. Am., 1986, pp. 351–378.
52. Koppers, A.A.P., Morgan, J.P., Morgan, J.W., et al., Testing the Fixed Hypothesis Using $^{40}Ar/Ar^{39}$ Age Progressions along Seamount Trails, *Earth Planet. Sci. Lett.*, 2001, vol. 185, pp. 237–252.
53. Langseth, M.G., Hobart, M.A., and Horai, K., Heat Flow in the Bering Sea, *J. Geophys. Res.*, 1980, vol. 85, pp. 3740–3750.
54. Mammerickx, J. and Sharman, G.F., Tectonic Evolution of the North Pacific during the Cretaceous Quiet Period, *J. Geophys. Res.*, 1988, vol. 93, no. B4, pp. 3009–3024.
55. Marlow, M.S., Cooper, A.K., Dadisman, S.V., et al., Bowers Swell: Evidence for a Zone of Compressive Deformation Concentric with Bowers Ridge, Bering Sea, *Mar. Petrol. Geol.*, 1990, vol. 7, no. 4, pp. 398–423.
56. Molnar, P. and Stock, J., Relative Motions of Hotspots in the Pacific, Atlantic and Indian Ocean since Late Cretaceous Time, *Nature*, 1987, vol. 327, pp. 587–591.
57. Muller, R.D., Royer, J.Y., and Lawver, L.A., Revised Plate Motions Relative to the Hotspots from Combined Atlantic and Indian Ocean Hotspot Tracks, *Geology*, 1993, vol. 21, no. 3, pp. 275–278.
58. Parsons, B. and Sclater, J.C., An Analysis of the Variation of Ocean Floor Bathymetry and Heat Flow with Age, *J. Geophys. Res.*, 1977, vol. 82, no. 5, pp. 803–827.
59. Pitman, W.C. and Talwani, M., Sea-Floor Spreading in the North Atlantic, *Bull. Geol. Soc. Amer.*, 1972, vol. 83, pp. 619–646.
60. Rea, D.K. and Dixon, J.M., Late Cretaceous and Paleogene Tectonic Evolution of the North Pacific, *Earth Planet. Sci. Lett.*, 1983, vol. 65, no. 1, pp. 145–166.
61. Renkin, M. and Sclater, G., Depth and Age in the North Pacific, *J. Geophys. Res.*, 1988, vol. 93, no. B4, pp. 2919–2935.
62. Richardson, K.R., Smallwood, J.R., White, R.S., et al., Crustal Structure beneath the Faroe Islands and the Faroe–Iceland Ridge, *Tectonophysics*, 1998, vol. 300, pp. 159–180.
63. Scholl, D.W., Buffington, E.C., and Marlow, M.S., Plate Tectonics and the Structural Evolution of the Aleitian–Bering Sea Region, in *Contributions to the Geology of the Bering Sea Basin and Adjacent Regions*, Forbes, R.B., Ed., *Spec. Pap. Geol. Soc. Amer.*, 1975, vol. 151, pp. 1–32.

along seamount trails // Earth Planet. Sci. Lett. 2001. V. 185. P. 237–252.

53. *Langseth M.G., Hobart M.A., Horai K.* Heat flow in the Bering Sea // J. Geophys. Res. 85. 1980. P. 3740–3750.
54. *Mammerickx J., Sharman G.F.* Tectonic evolution of the North Pacific during the Cretaceous Quiet Period // J. Geophys. Res. 1988. V. 93. № B4. P. 3009–3024.
55. *Marlow M.S., Cooper A.K., Dadisman S.V. et al.* Bowers swell: evidence for a zone of compressive deformation concentric with Bowers Ridge, Bering Sea // Mar. Petrol. Geol. 1990. V. 7. № 4. P. 398–423.
56. *Molnar P., Stock J.* Relative motions of hotspots in the Pacific, Atlantic and Indian Ocean since late Cretaceous time // Nature. 1987. V. 327. P. 587–591.
57. *Muller R.D., Royer J.Y., Lawver L.A.* Revised plate motions relative to the hotspots from combined Atlantic and Indian Ocean hotspot tracks // Geology. 1993. V. 21. № 3. P. 275–278.
58. *Parsons B., Sclater J.C.* An analysis of the variation of ocean floor bathymetry and heat floor with age // J. Geophys. Res. 1977. V. 82. № 5. P. 803–827.
59. *Pitman W.C., Talwani M.* Sea-floor spreading in the North Atlantic // Bull. Geol. Soc. Amer. 1972. V. 83. P. 619–646.
60. *Rea D.K., Dixon J.M.* Late Cretaceous and Paleogene tectonic evolution of the North Pacific // Earth Planet. Sci. Lett. 1983. V. 65. № 1. P. 145–166.
61. *Renkin M., Sclater G.* Depth and age in the North Pacific // J. Geophys. Res. V. 93. № B4. 1988. P. 2919–2935.
62. *Richadson K.R., Smallwood J.R., White R.S. et al.* Crustal structure beneath the Faroe Islands and the Faroe-Iceland Ridge // Tectonophysics. 1998. V. 300. P. 159–180.
63. *Scholl D.W., Buffington E.C., Marlow M.S.* Plate tectonics and the structural evolution of the Aleution-Bering Sea region // Forbes R.B. (ed.) Contributions to the Geology of the Bering Sea Basin and Adjacent Regions. // Spec. Pap. Geol. Soc. Am. 1975. V. 151. P. 1–32.
64. *Scholl D.W., Creager J.S.* Geologic synthesis of Leg 19 (DSDP) results: Far North Pacific, Aleutian Ridge and Bering Sea // Initial Rep. Deep Sea Drill. Proj. 1973. V. 19. P. 897–913.
65. *Scholl D.W., Hein J.R., Marlow M. et al.* Meiji sediment tongue: North Pacific evidence for limited movement between the Pacific and North American plates // Geol. Soc. Amer. Bull. 1977. V. 88. № 11. P. 1567–1576.
66. *Scholl D.W., Vallier T.L., Stevenson A.J.* Geologic evolution and petroleum geology of the Aleution Ridge // Geology and Resource Potential of the Continental Margin of Western North America and Adjacent Ocean Basin – Beaufort Sea to Baja California // Earth Sci. Ser. 1987. V. 6. P. 123–155.
67. *Scotese C.R., Nokleberg W.J., Monger J.W.H. et al.* Dynamic Computer Model for the Metallogenesis and Tectonics of the Circum-North Pacific / Eds. Nokleberg W.J., Diggles M.F. Open-File Report 01-261. 2001. Version 1.0. CD-ROM.
68. *Woods M.T., Davies, G.F.* Late Cretaceous genesis of the Kula plate // Earth Planet. Sci. Lett. 1982. V. 58. P. 161–166.
69. *Zonenshain L.P., Savostin L.A., Baranov B.V.* Plate boundaries of the USSR// Episodes. 1984. V. 7. P. 43.
70. *Zonenshain L.P., Pristavakina E.I., Kononov M.V., Baranov B.V.* Plate tectonic reconstructions of the Arctic region: a Russian perspective // Cambridge Arctic Shelf Programme (CASP). Report № 595. 1994. 89 p.

Geothermal Regime and Geodynamics of the North Pacific Ocean

E. V. Verzhbitskii[1], M. V. Kononov[1], V. D. Kotelkin[2]

[1] *Institute of Oceanology, Russian Academy of Sciences, Moscow, 117997, Russia*

[2] *Faculty of Mechanics and Mathematics, Moscow State University, Moscow, 119899, Russia*

The distribution of heat flow in the North Pacific Ocean has been examined, and a map of geothermal and geomagnetic fields for the Bering Sea as it is known today has been made. Reliable data are lacking as to the time of origin for features of oceanic and continental genesis for the Bering Sea, which is an obstacle in the way of studying geodynamic processes in the North Pacific. Heat flow data were used to yield numerical estimates for the age of seafloor features in the Bering Sea: the Kamchatka Basin (21 Ma), Shirshov Ridge (95 Ma for the northern part and 33 Ma for the southern), the Aleutian Basin (70 Ma), Vitus Arch (44 Ma), Bowers Ridge (30 Ma), and Bowers Basin (40 Ma). These age estimates are corroborated by combined geological, geophysical, and plate kinematic data. A thermal-chemical model of global mantle convection was used to perform a numerical simulation of the thermal process involved in the generation of extended regional features in the North Pacific (the Emperor Trough, Chinook Trough, etc.). The modeling suggests a plume-tectonic origin for these features. An integrated geological and geothermal analysis leads to the conclusion that the northern and southern parts of the Shirshov Ridge are different, not only in geological age, but also in tectonic structure. The northern part is characterized by imbricated-thrust terrain nature, while the southern part is of ensimatic island-arc origin similar to that of Bowers Ridge. The bottom of the Aleutian Basin is an autlier of the Upper Cretaceous Kula plate where, in the Vitus Rise area, backarc spreading processes originated dirung Eocene time. The terminating phase of activity in the Bering Sea began about 21 Ma by spreading in the older seafloor of the Kamchatka Basin. We developed plate-tectonic reconstructions of evolution for the North Pacific for the times 21, 33, 40, and 70 Ma in the hot-spot system based on age estimates for the seafloor features derived from heat flow data, the modeling of the thermal generation of regional faults, as well as on an analysis of geomagnetic, tectonic and geological data.